Adsorption Kinetics of CO_2, O_2, N_2, and CH_4 in Cation-Exchanged Clinoptilolite

Gelacio Aguilar-Armenta,*,† Guadalupe Hernandez-Ramirez,† Erika Flores-Loyola,† Alejandra Ugarte-Castaneda,† Rutilo Silva-Gonzalez,‡ Cristobal Tabares-Munoz,‡ Antonio Jimenez-Lopez,§ and Enrique Rodriguez-Castellon§

Centro de Investigacion de la Facultad de Ciencias Quimicas, Benemerita Universidad Autonoma de Puebla, Bvd. 14 Sur y Av. San Claudio, C.U., Col. San Manuel, C.P. 72570, Puebla, Puebla, Mexico, Instituto de Fisica "Luis Rivera Terrazas", Benemerita Universidad Autonoma de Puebla, Ado. Postal J-48, Col. San Manuel, C.P. 72570, Puebla, Puebla, Mexico., and Dpto de Quimica Inorganica, Facultad de Ciencias, Universidad de Malaga, 29071 Malaga, Spain

Received: September 24, 1999; In Final Form: November 7, 2000

The rate of adsorption of pure CO_2, O_2, N_2, and CH_4 on natural untreated clinoptilolite-rich volcanic tuff (Cp) from Tehuacan (Puebla, Mexico), and on cation-exchanged clinoptilolite samples (Ca−Cp, K−Cp, and Na−Cp) has been measured at 20 °C using a glass high-vacuum volumetric apparatus. The X-ray diffraction pattern of Cp showed that the main crystalline phases correspond to clinoptilolite-heulandite and minor amounts of mordenite, cristobalite, feldspar (albite), quartz, smectite, and opal. The adsorption rates of gases in the initial period ($t < 180$ s) were measured with a custom acquisition data card capable of registering pressure and time data five times per second, simultaneously. The influence of cation exchange on adsorption kinetics of the gases depended on the gas-adsorbent contact time (t). In the initial period, the adsorption rate of all gases on all samples decreased in the order Ca−Cp > K−Cp > Cp > Na−Cp, and the affinity decreased in the order $CO_2 \gg N_2 > O_2 > CH_4$, whereas at equilibrium ($t \rightarrow \infty$ s) the adsorption uptake decreased in the sequence $CO_2 \gg CH_4 > N_2 > O_2$. The slow adsorption of methane in Na−Cp was probably due to diffusional difficulties as a result of channel blockage by Na^+ cations. By cation exchange of Cp an adsorbent can be tailored for the separation of N_2/O_2, N_2/CH_4, and CO_2/CH_4 mixtures.

Introduction

Zeolites are porous, crystalline, hydrated aluminosilicates of alkali and alkaline earth cations that possess a three-dimensional structure. The zeolite framework consists of an assemblage of SiO_4 and AlO_4 tetrahedra joined together in various regular arrangements through shared oxygen atoms to form an open crystal structure containing pores of molecular dimensions into which guest molecules can penetrate. The negative charge created by the substitution of an AlO_4 tetrahedron for a SiO_4 tetrahedron is balanced by exchangeable cations (e.g., Na^+, K^+, Ca^{2+}, Mg^{2+}), which are located in large structural channels and cavities throughout the structure. These cations play a very important role in determining the adsorption and gas-separation properties of zeolites. These properties depend heavily on the size, charge density, and distribution of cations in the porous structure. Synthetic zeolites are manufactured on a large scale for industrial use, but natural zeolites have not yet found extensive application as commercial molecular sieves, even though a few, particularly clinoptilolite, are abundant in volcanogenic sedimentary rocks.[1] Of the more than 40 natural zeolites species known today, clinoptilolite is the most abundant in soils and sediments. The framework of clinoptilolite is formed by two parallel channels of 10-member rings (channel A) and eight-member rings (channel B) connected to a third channel C of eight-member rings.[1] The approximate channel sizes (Å) are: A, 4.4 × 7.2; B, 4.1 × 4.7; C, 4.0 × 5.5. Small hydrated cations (Na^+, K^+, Ca^{2+}, and Mg^{2+}) can easily enter the channels of clinoptilolite and compete for the major exchangeable-cation sites,[2] designated as M(1), M(2), M(3), and M(4). The major cations are located and distributed as follows:[3] M(1) is located in channel A, where Na > Ca; M(2) is located in channel B, where Ca > Na; M(3) is located in channel C, where there is only K; and M(4) is located in channel A, where there is only Mg. Clinoptilolite has been applied to gas and radioactive wastewater cleaning, gas separation, and gas drying,[4−6] and Minato et al.[7] and Galabova et al.[8] discussed the possibility of using clinoptilolites to separate oxygen from air. Others[9,10] have shown that the use of K-exchanged clinoptilolite for air separation leads to an increase in the coefficient of oxygen production. Frankiewicz and Donnelly[11] found that clinoptilolite can be used to separate N_2/CH_4 mixtures, and that an incompletely exchanged sample containing divalent cations appeared to be the most selective for N_2. Through cation manipulation, Ackley et al.[12] tailored clinoptilolite for a commercially viable, kinetic separation of a N_2/CH_4 mixture. The affinity of zeolites for N_2 is attributable to the field gradient−quadrupole interaction energy,[13,14] which is stronger for divalent cations than for monovalent cations. Boniface et al.[15] reported that clinoptilolite appeared to be a promising adsorbent for O_2/Ar separation, but because O_2 is preferentially adsorbed, this adsorbent was not ideal for purifying oxygen. Mumpton[16] noted that natural zeolites, primarily chabazite and clinoptilolite, have been used to purify natural gas contaminated with large amounts of CO_2, H_2S, and H_2O.

In view of the fact that large deposits of zeolitic tuffs,

* Author to whom correspondence should be addressed. Fax: 52 22 295 584. E-mail: geaguila@siu.buap.mx.

† Centro de Investigacion de la Facultad de Ciencias Quimicas, Benemerita Universidad Autonoma de Puebla. Fax: 52 22 295 584.

‡ Instituto de Fisica "Luis Rivera Terrazas", Benemerita Universidad Autonoma de Puebla. Fax: 52 22 448 947.

§ Dpto de Quimica Inorganica, Facultad de Ciencias, Universidad de Malaga. Fax: 34 52 132000.

10.1021/jp9934331 CCC: $20.00
Published on Web 01/26/2001

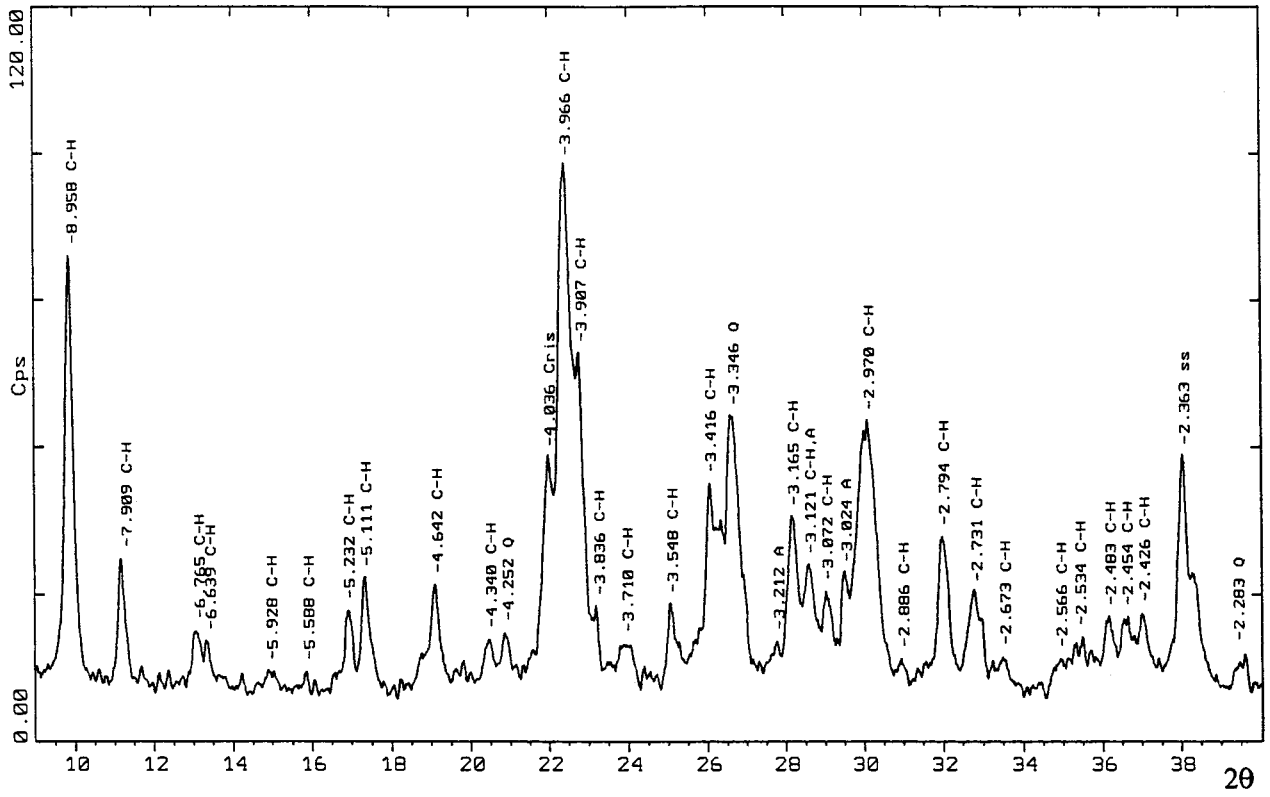

Figure 1. X-ray powder diffraction pattern of Cp sample. **C**, Clinoptilolite; **H**, Heulandite; **A,** Albite (feldspar); **Cris**, Cristobalite; **M**, Mordenite; **Q**, Quartz; **ss**, sample support.

TABLE 1: Chemical Composition (weight %) of Untreated and Cation-Exchanged Clinoptilolite-Rich Tuff from Tehuacan, Puebla (Mexico)

sample[a]	K	Na	Ca	Mg	Si	Al	Si/Al	Ti	Fe
Cp	1.90	1.70	0.76	0.48	27.71	4.42	6.27	0.30	0.69
Na−Cp	0.40	3.78	0.20	0.45	28.00	4.46	6.28	0.20	0.42
K−Cp	4.65	0.00	0.00	0.48	29.00	4.70	6.17	0.10	0.24
Ca−Cp	1.98	0.00	2.71	0.46	28.87	4.61	6.26	0.15	0.35

[a] Cp denotes the natural untreated clinoptilolite-rich volcanic tuff. The Na−Cp, K−Cp, and Ca−Cp samples were prepared by aqueous exchange of the Cp sample with sodium, potassium, and calcium chloride solutions, respectively.

primarily of clinoptilolite, have been discovered in Mexico, we began an investigation of the adsorption properties of these materials to evaluate their possible industrial applications, e.g., in gas separation processes. The particular objective of this study was to investigate the influence of cation exchange of natural clinoptilolite (Cp) (using aqueous solutions of salts NaCl, KCl, and $CaCl_2$) on the adsorption kinetics of CO_2, O_2, N_2, and CH_4 at 20 °C.

Experimental Section

To simplify the notation, the untreated clinoptilolite-rich volcanic tuff is referred to below as Cp; Na−Cp, K−Cp, and Ca−Cp denote the cation-exchanged clinoptilolite samples.

Characterization of Samples. *Methods*. The X-ray powder diffraction (XRD) pattern of Cp was obtained on a Siemens D-5000 diffractometer using CuKα radiation ($\lambda = 1.5406$ Å), a step size of 0.02° 2θ and a counting time of 4.0 s/step. The XRD pattern showed (Figure 1) that the main crystalline phases correspond to a clinoptilolite-heulandite mineral[17] and lesser amounts of mordenite, cristobalite, feldspar (albite), quartz, smectite, and opal. The chemical composition (Table 1) of the samples was obtained by means of a standardless method

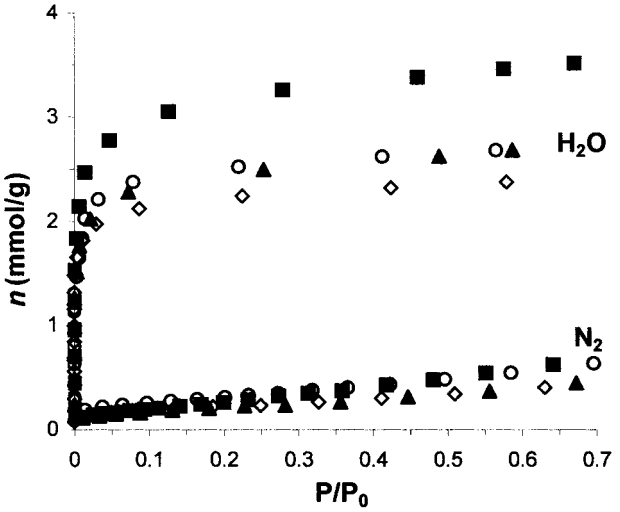

Figure 2. Adsorption isotherms of H_2O (20 °C) and N_2 (77 K). ■ Ca−Cp, ○ Cp, ▲ K−Cp, ◇ Na−Cp.

Voyager 2100 and an energy-dispersive X-ray spectrometer (Voyager-Noran), coupled to a scanning electron microscope (JEOL-JSM-5400 LV). To obtain a more representative chemical composition of the sample bulk, the analysis was done on 10 different grains of each sample, and the element contents were averaged (Table 1). These data show that the Cp sample exhibits cation selectivity; e.g., Na^+ and Ca^{2+} were entirely replaced by K^+, but Ca^{2+} and K^+ were only partially replaced by Na^+. From Table 1 it can also be seen that Na^+ was fully replaced by Ca^{2+}.

The samples were also characterized by the classical N_2-adsorption method at 77 K and water adsorption at 20 °C (Figure 2) in a glass high-vacuum volumetric system. The low adsorption of N_2 at 77 K on Cp and on the exchanged samples (Ca−

TABLE 2: Surface area (S) and Micropore Volume (V_o) of Untreated and Cation-Exchanged Clinoptilolite-Rich Tuff from Tehuacan, Puebla (Mexico)

	S (m^2/g)		V_o[a] (cm^3/g)
sample[b]	BET	Lang.	DA
Cp	25	28	0.0506
Na−Cp	18	21	0.0480
K−Cp	17	17	0.0500
Ca−Cp	25	17	0.0650

[a] H_2O adsorption, Dubinin-Astakhov ($n = 1$). [b] Sample abbreviations are as in Table 1.

Cp, K−Cp, Na−Cp) was probably due to kinetic effects, i.e., at 77 K nitrogen molecules diffused into micropores with considerable difficulty and even after more than 8 h did not attain adsorption equilibrium. The samples gave type-IV N_2-adsorption isotherms, and the BET model described the experimental points up to $P/P_o \leq 0.40$ perfectly. The Langmuir model was able to fit the adsorption isotherms only over the range $0.01 \leq P/P_0 \leq 0.10$. Unlike the N_2 adsorption isotherms, H_2O adsorption isotherms were of type I; thus, the molecules of H_2O were able to penetrate freely into the micropores. The micropore volume[18,19] (Dubinin-Astakhov) of samples decreased in the order: Ca−Cp > Cp ≈ K−Cp > Na−Cp (Table 2).

Ion Exchange. The Na−Cp, K−Cp, and Ca−Cp samples were prepared by aqueous exchange of Cp with sodium, potassium, and calcium chloride solutions at 0.5 N concentration. Before each cation-exchange treatment, the Cp was washed with distilled water to eliminate soluble impurities. One gram (fraction 20−30 mesh) of Cp was placed in a 1.4-cm diameter glass ion-exchange column of 12-cm length and held at 65 °C. Subsequently, 200 mL of solution was percolated through the samples for 30 min. This cation-exchange procedure was repeated twice. After the cation-exchange treatment the samples were thoroughly washed with distilled water until the filtrate was free of chloride ions. To evaluate the success of the cation-exchange process, the exchange treatment was repeated. After four additional cation-exchange treatments, the Na content increased by only 1.8% absolute.

Adsorption Kinetics Measurement. The adsorption of CO_2, O_2, N_2, and CH_4 as a function of time t was obtained by the volumetric method on the basis of the difference between the initial amount of gas introduced into the cell and the amount of gas remaining in the dead space of the cell at any given time t_i, from $t = 0$ until $t = \infty$ (equilibrium). In all experiments, the initial pressure was 450 Torr (600 mb). The high-vacuum system was made of Pyrex glass, which was equipped with grease-free valves and calibrated with He. The vacuum was created by a turbomolecular pump (TSH 062, Balzers) capable of establishing pressure $< 10^{-7}$ Torr. The pressures were measured by two types of pressure transducers (Balzers) of different range: TPR 017 (10^{-4}−5 Torr) and APR 011 (1−1000 Torr). About 500 mg of each sample were first dehydrated in situ at 280−320 °C in an oven up to a residual pressure of $< 6 \times 10^{-4}$ Torr. After sample dehydration, the temperature was decreased to the desired point at which time the sample was allowed to stabilize for at least 1.5 h before the beginning of the measurement. To analyze in detail the sudden drop in pressure that occurred when the gases were put into contact with the adsorbents, a custom acquisition data card was used which allows simultaneous monitoring and recording of time and pressure. In the period 0−3 min, pressure was monitored five times per second because this initial period is the most important period in gas separation processes, such as the pressure swing adsorption method (PSA). Afterward, in the period 3−13 min, pressure was registered once per second, and pressure was recorded once every 10 seconds in the period 13−∞ min.

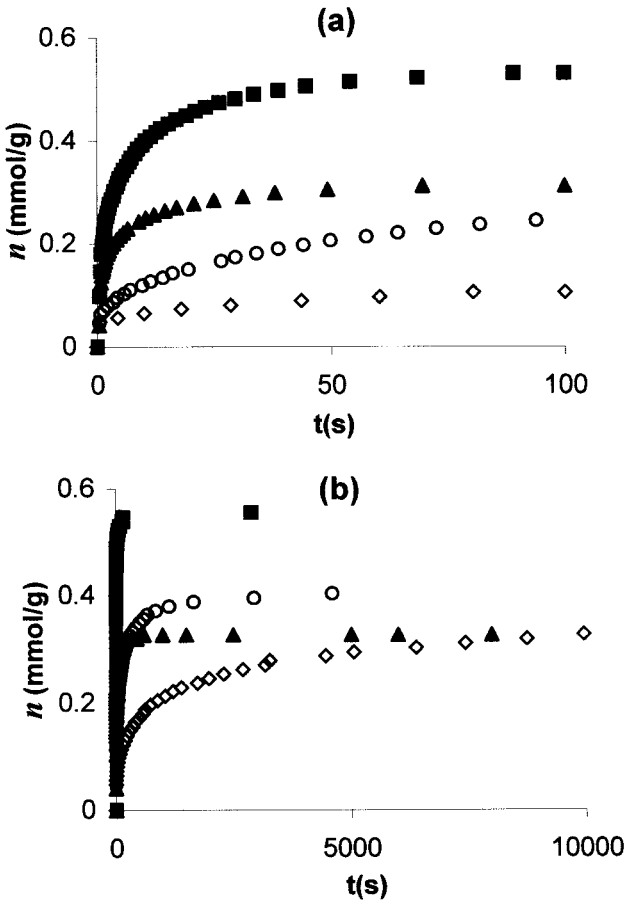

Figure 3. Adsorption uptake of N_2. ■ Ca−Cp, ○ Cp, ▲ K−Cp, ◇ Na−Cp.

The size and polarizing power of the cations present in the zeolite channels may influence the selective adsorption of certain molecules, and the adsorptive properties of a heteroionic natural zeolite that is converted to a near homoionic form, should therefore change. In the next section the adsorption uptake curves of each gas are shown separately. From differences in adsorption kinetic behavior of the gases, we propose what appears to be the best sample for the separation of certain binary gas mixtures.

Results

Adsorption Kinetics of Pure Gases. Figures 3, 4, 5, and 6 show the adsorption uptake of N_2, O_2, CH_4, and CO_2, respectively, both for short ($t \leq 100$ s) (a) and long ($t \rightarrow \infty$) (b) gas-adsorbent contact times**.** These figures show the marked influence of cation type on the adsorption uptake of all gases, especially for short contact times. To evaluate the effect of cation-exchange, the adsorption uptake by the untreated sample (Cp) is also included in these figures. In the initial uptake region ($t \leq 100$ s), the adsorption rate decreased in the following order Ca−Cp > K−Cp > Cp > Na−Cp. For the Cp and K−Cp samples, the uptake curves (see Figures 4a, and 6a) of O_2 and CO_2 were very similar. At equilibrium, however, the adsorption uptake of gases behaved as follows: for CO_2: Ca−Cp ≈ Cp ≈ Na−Cp > K−Cp; for O_2: Ca−Cp > Cp ≈ K−Cp ≈ Na−Cp; for N_2: Ca−Cp > Cp > K−Cp ≈ Na−Cp; for CH_4: Ca−Cp ≈ K−Cp ≫ Cp > Na−Cp. The adsorption rate of these gases in the initial uptake region ($t < 100$ s) on all samples,

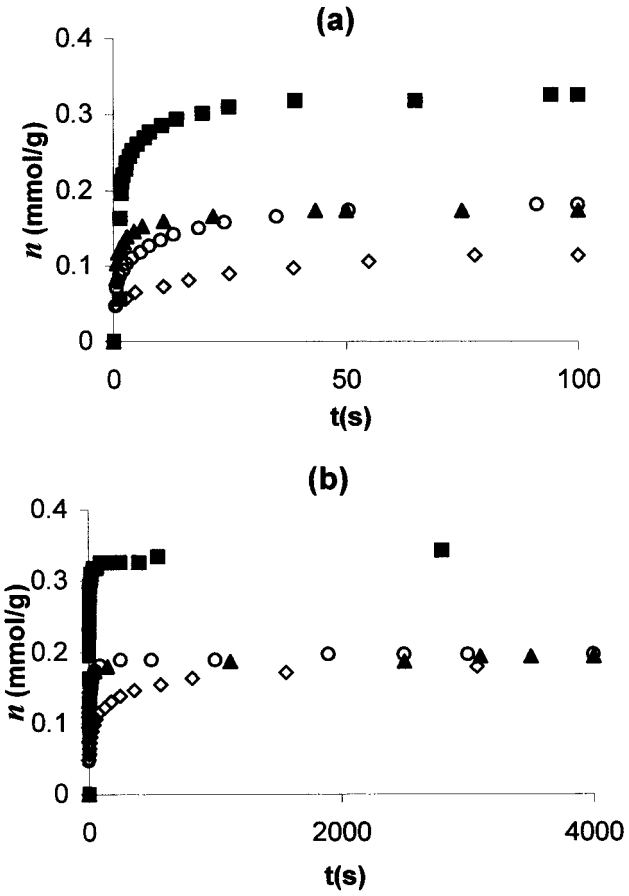

Figure 4. Adsorption uptake of O_2. ■ Ca−Cp, ○ Cp, ▲ K−Cp, ◇ Na−Cp.

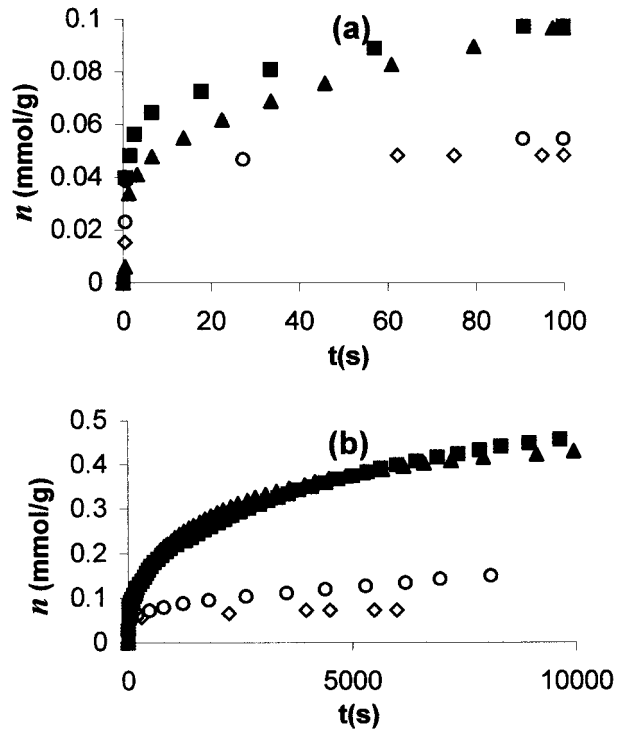

Figure 5. Adsorption uptake of CH_4. ■ Ca−Cp, ○ Cp, ▲ K−Cp, ◇ Na−Cp.

and for the Cp and Na−Cp samples for $t \rightarrow \infty$, decreased in the order $CO_2 \gg N_2 > O_2 > CH_4$. However, the adsorption uptake for $t \rightarrow \infty$ behaved in the following way for Ca−Cp:

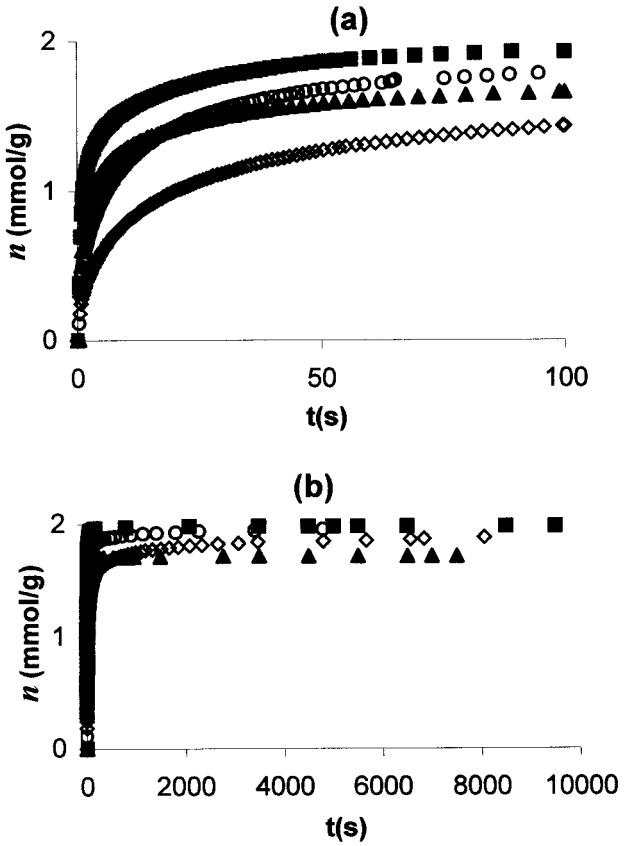

Figure 6. Adsorption uptake of CO_2. ■ Ca−Cp, ○ Cp, ▲ K−Cp, ◇ Na−Cp.

$CO_2 \gg N_2 \approx CH_4 > O_2$, and for K−Cp: $CO_2 \gg CH_4 > N_2 > O_2$. The fact that for Cp and Na−Cp samples, which contain Na^+ cations (Table 1), the adsorption uptake decreased in the order $CO_2 \gg N_2 > O_2 > CH_4$ both for short and long gas-adsorbent contact times, suggests that the Na^+ cations occupied positions in the zeolite structure that caused diffusional restrictions to the larger CH_4 molecule. CO_2 had the highest affinity of the adsorbates studied in all clinoptilolite samples because of strong ion−quadrupole interactions.[20]

Adsorption Kinetics of Gas Pairs. *(a) N_2/O_2.* Figure 7 compares the adsorption kinetic behavior of N_2 and O_2 in different cation-exchanged samples with the corresponding kinetic behavior of the Cp sample. Interestingly, the adsorption uptake of O_2 on Cp in the region $t \leq 20$ s was close to that of N_2 (Figure 7a). For the Na−Cp sample, this effect was the same until $t \leq 120$ s. Furthermore, the adsorption uptake of both gases by this sample was lower than by Cp. Unlike the results for the Na−Cp sample, the amounts of both gases adsorbed by the K−Cp and Ca−Cp samples were greater than for Cp, especially for the Ca−Cp sample. The uptake of N_2 was greater than that of O_2 in all samples, due to the higher quadrupole moment of N_2 compared with that of O_2. The difference in the adsorption uptake suggests that the Ca−Cp and K−Cp samples could be used for O_2 enrichment from air. By virtue of the greater difference between the uptake curves of N_2 and O_2 for Ca−Cp, compared with K−Cp, Ca−Cp would probably be the best material for O_2 enrichment from air.

(b) N_2/CH_4. Figure 8 shows that samples Ca−Cp, K−Cp, and Cp were highly selective for N_2 over CH_4. The selectivity for N_2 decreased in the order Ca−Cp > K−Cp > Cp ≫ Na−Cp, i.e., the Ca−Cp sample seemed to be the most suitable for the separation of this gas mixture. However, because CH_4 adsorption on K−Cp and Ca−Cp samples increased slowly with

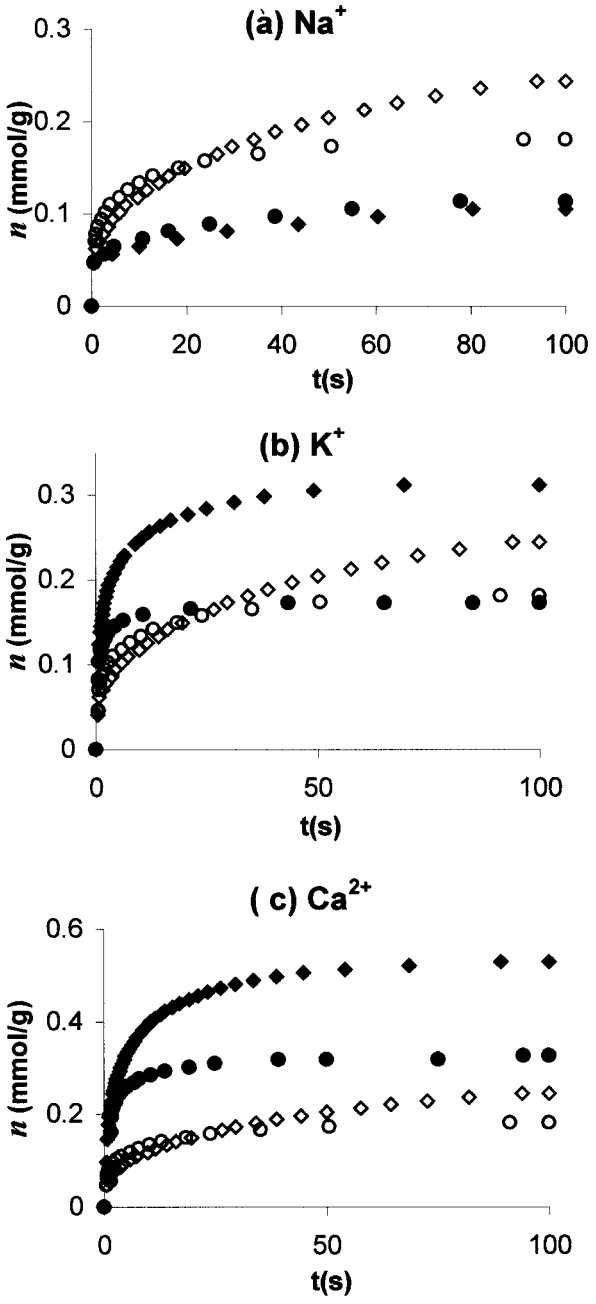

Figure 7. Adsorption uptake of the N_2/O_2 pair. ◇ N_2, ○ O_2, Cp; ◆ N_2, ● O_2, Na−Cp, K−Cp, Ca−Cp.

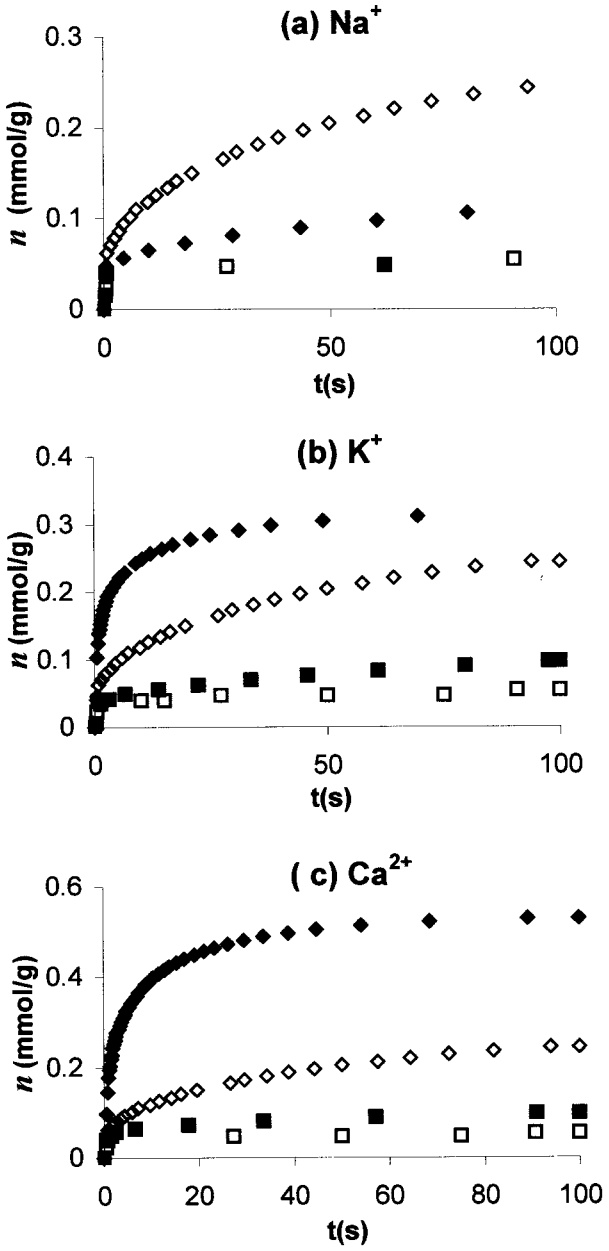

Figure 8. Adsorption uptake for N_2/CH_4. ◇ N_2, □ CH_4, Cp; ◆ N_2, ■ CH_4, Na−Cp, K−Cp, Ca−Cp.

time, reaching the N_2 adsorption of Ca−Cp and exceeding the N_2 adsorption of K−Cp at equilibrium, these samples are not recommended for purifying N_2 contaminated with CH_4, at long gas-contact times. These results coincide with those reported by other authors[13] for K^+-clinoptilolite. CH_4 adsorption on these samples was probably determined by diffusive restrictions in micropores, principally in the Na−Cp sample. Therefore, the adsorptive separation of this gas mixture can be achieved by virtue of differences in diffusion rates of these molecules.[21]

(c) CO_2/CH_4. As indicated above, CO_2 had the highest affinity in all samples, a fact that is attributable to the specific interactions of the CO_2 quadrupole with the electric field created by the cations in the zeolite structure. Thus, if the CO_2/CH_4, CO_2/O_2, and CO_2/N_2 mixtures were contacted with any of the four studied clinoptilolite samples, CO_2 would be adsorbed preferentially, leading to a purification of these gases. Figure 9 shows that for short contact times (t < 100 s), Ca−Cp would be the most effective of the lot for separation of the CO_2/CH_4 mixture, whereas at equilibrium the Na−Cp sample would have the highest efficiency, because the CH_4 adsorption in this sample was negligible.

Discussion

To interpret the results, the chemical composition (Table 1) and crystal structure of the adsorbents must be considered, as well as the fundamental properties of the exchanged cations[22−24] (Table 3) and the adsorbate molecules[25] (Table 4). Chemical analyses reveal that untreated Cp was rich in alkali (Na, K) and poor in alkaline-earth metals (Ca, Mg). The most noticeable feature of the cation-exchange process was the high selectivity of clinoptilolite for K^+ cations, which is in accord with the results of other authors[3,11,26]. The uptake rate of the gases in the initial region ($t \leq 100$ s), decreasing in the order Ca−Cp > K−Cp > Cp > Na−Cp, correlates with the Ca^{2+} and Na^+ contents in the zeolitic channels, and the highest adsorption rate

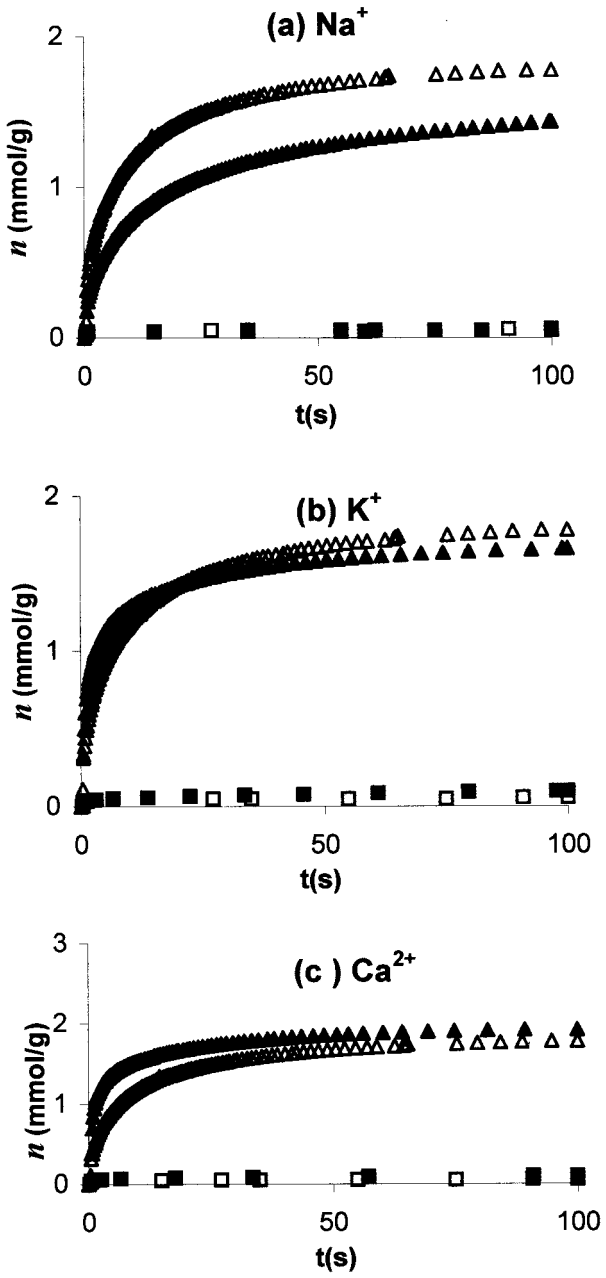

Figure 9. Adsorption uptake for CO_2/CH_4. △ CO_2, □ CH_4, Cp; ▲ CO_2, ■ CH_4, Na−Cp, K−Cp, Ca−Cp.

TABLE 3: Properties of Exchangeable Cations[22−24] [a]

	r (Å)	E	$\Phi = Z/r$
Na^+	0.95	0.93	1.05
K^+	1.33	0.82	0.75
Ca^{2+}	0.99	1.00	2.02

[a] r, ionic radii; E, electronegativity (Pauling); Φ, ionic potential.

occurred for a zeolite that had more Ca^{2+} and less Na^+. The fact that the uptake curve for Cp was situated above the Na−Cp curve may be due to the higher Ca^{2+} and lower Na^+ content of the untreated Cp compared with Na−Cp (Table 1).

To evaluate the adsorption rate of each gas, the time required to occupy half of the total adsorption capacity (n_∞) was evaluated. This time ($t_{1/2}$) corresponds to the relationship $n_t/n_\infty = 0.5$, where n_t and n_∞ are the uptake at time t and t_∞ (equilibrium), respectively. The values of $t_{1/2}$ (Table 5) show that CH_4, with the largest kinetic diameter (Table 4), is adsorbed more slowly than the other gases, perhaps due to diffusive

TABLE 4: Physical Constants of Gases[25] [a]

	σ (Å)	μ (Å^3)	α (Å^3)
N_2	3.64	0.31	1.4
O_2	3.46	0.10	1.2
CH_4	3.80	0	2.6
CO_2	3.30	0.64	1.9

[a] σ, kinetic diameter; α, polarizability; μ, quadrupolar moment.

TABLE 5: Values of $t_{1/2}$ (s) to Attain 50% Equilibrium

sample[a]	CO_2	O_2	N_2	CH_4
Cp	6	2.8	48	680
Na−Cp	16	25	405	<1
K−Cp	1.8	<1	1.7	1200
Ca−Cp	1.2	1.6	2.8	1900

[a] Sample abbreviations are as in Table 1.

restrictions in the zeolite channels. Apparently, the instantaneous adsorption of CH_4 on the Na−Cp sample (Table 5) was due to the inability of the CH_4 molecule to enter the zeolite channels and, consequently, this gas was adsorbed only on the external surface of the Na−Cp sample. This supposition is supported by the fact that for this sample, the values of $t_{1/2}$ for the other three gases increased in the sequence $CO_2 < O_2 < N_2$ (Table 5), in order of the increasing size of these molecules (Table 4). Given the $t_{1/2}$ value of 16 s for Na−Cp with CO_2, which has the lowest kinetic diameter of the gases studied, it is likely that the very low value of $t_{1/2}$ (<1 s) measured for the CH_4 molecule suggests that in fact the micropores did not take part in the adsorption of CH_4 on this sample. From the CH_4 adsorption uptake behavior at 0 °C and 20 °C, the $t_{1/2}$ value apparently did not depend on temperature and, therefore, the activation energy (E_a) was equal to zero. This means that the adsorption of CH_4 in this temperature range (0−20 °C) was not controlled by a diffusion process. Likewise, for the other three samples, a diffusion process did not control CH_4 adsorption.

Figure 10 compares the adsorption uptake behavior of N_2 and CH_4 on the Ca−Cp and K−Cp samples. Note that the time required to reach total CH_4 uptake (n_∞) for these samples was about 5 h. Note also that the n_∞ value for CH_4 reached and overcomes n_∞ for N_2 on the Ca−Cp and K−Cp samples, respectively. If the CH_4 molecule enters the zeolite micropore structure freely, as in natural erionite,[27] then the adsorption uptake of CH_4, according to the polarizability of the gases, would be greater than for N_2 at any gas-adsorbent contact times. Accordingly, the fact that the N_2 adsorption uptake on all samples was greater than for CH_4 at short times, as well as for the Cp and Na−Cp samples at equilibrium, suggests that the location of cations in the channels of clinoptilolite plays a very important role. Moreover, from the fact that CH_4 adsorption uptake reached and overcame N_2 adsorption uptake for Ca−Cp and K−Cp, respectively, it can be supposed that the channel blockage factor decreased in the following order: Na ≫ Ca > K. Thus, the lower gas adsorption, especially for CH_4, shown for Na−Cp sample at low contact times, can be attributed to the reduction of effective channel aperture sizes by Na^+ cations. This supposition is supported by the $t_{1/2}$ values for CO_2, O_2, and N_2 (Table 5) decreasing in the sequence Na−Cp > Cp, i.e., in order of the decreasing content of Na^+ cations (Table 1), and by the fact that the $\Delta t_{1/2}(s) = t_{1/2}(Na-Cp) - t_{1/2}(Cp)$ for each gas increased as follows: CO_2 (10) < O_2 (22) < N_2 (357), i.e., in the order of the increasing kinetic diameter of molecules (Table 4). The similar adsorption uptake of N_2 and O_2 on the Na−Cp and Cp samples at low gas-adsorbent contact times (Figure 7a) could be due to the greater influence of channel blockage by the Na^+ cations on the diffusion of N_2,

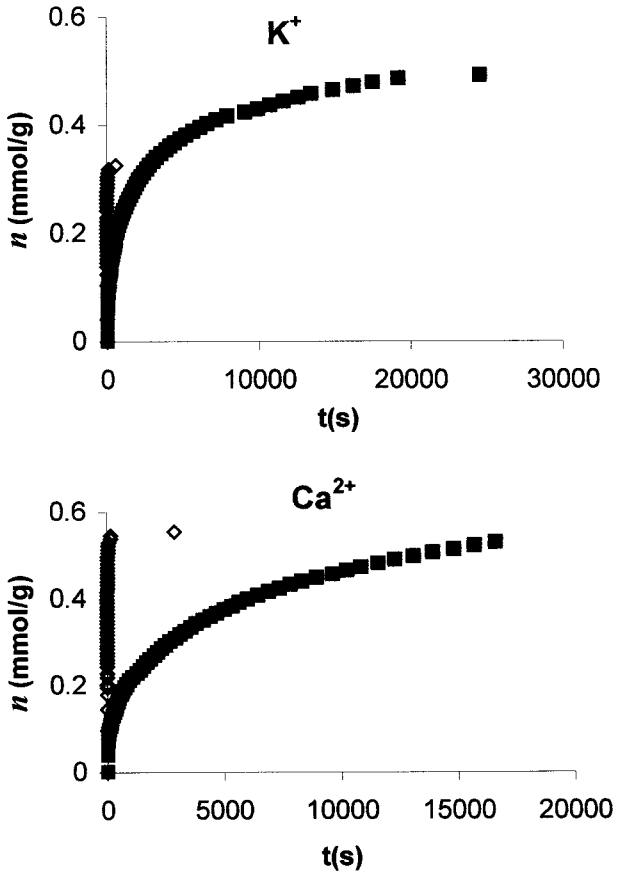

Figure 10. Adsorption uptake for N_2 and CH_4. ◇ N_2, ■ CH_4.

which is larger than O_2. In contrast to the CH_4 adsorption kinetic behavior, O_2, N_2, and CO_2 adsorption occurred quickly on K−Cp and Ca−Cp samples.

To understand the adsorption kinetic behavior of other gases, the CO_2 adsorption kinetic behavior was used as reference, inasmuch as this molecule is smaller and has the greatest polarizability and quadrupole moment in comparison with N_2, O_2, or CH_4. The CO_2 molecule is best suited[28] as an acidic probe to characterize the basicity of the zeolites. Figure 6a shows that the basicity increased from Na−Cp to Ca−Cp. In other words, if Na^+ and K^+ were replaced by Ca^{2+}, the basicity of the basic centers (i.e., framework oxygens) increased, which is consistent with the higher electronegativity of Ca^{2+} (Table 3). The sequence of increasing basic character Na−Cp < K−Cp at low gas−adsorbent contact times (Figure 6a) is somewhat puzzling because it is not consistent with other cation characteristics (electronegativity, ionic potential). However, for long gas-adsorbent contact times, as expected, the basic character increases in the order $K^+ < Na^+ < Ca^{2+}$. Figures 3b, 4b, 5b, and 6b show that the time (s) required for the adsorption uptake of each gas on Na−Cp to reach the adsorption uptake level on K−Cp increased in the following order CO_2 (500) < O_2 (3000) < N_2 (8000) < CH_4 (never), correlating fairly well with the increasing order of kinetic diameter (Å) of molecules: CO_2 (3.3) < O_2 (3.46) < N_2 (3.64) < CH_4 (3.8). Obviously, the reduction of effective channel apertures by Na^+ cations greatly influenced the adsorption of CH_4.

Summary

The cation exchange of natural clinoptilolite-rich tuff (Cp) with NaCl, KCl, and $CaCl_2$ aqueous solutions substantially influenced the adsorption kinetics of CO_2, O_2, N_2, and CH_4. In the initial uptake region ($t \leq 100$ s), the adsorption rate of all four gases on the studied samples decreased in the order: Ca−Cp > K−Cp > Cp > Na−Cp. The adsorption uptake on all samples in the initial period ($t \leq 100$ s), as well as for Cp and Na−Cp at equilibrium ($t \rightarrow \infty$), decreased in the order $CO_2 \gg N_2 > O_2 > CH_4$. For Ca−Cp and K−Cp, however, the selectivity at equilibrium decreased in the sequences: $CO_2 \gg N_2 \approx CH_4 > O_2$ and $CO_2 \gg CH_4 > N_2 > O_2$, respectively. The slow adsorption of CH_4 was probably due to diffusive restrictions in zeolite channels, which was principally the result of channel blockage by Na^+ cations. The influence of this blockage on the adsorption rate decreased with decreasing kinetic diameter of the gas molecules.

Based upon the results of this study, cation exchange of Cp could possibly be tailored to produce an adsorbent for the separation of N_2/O_2, N_2/CH_4, and CO_2/CH_4 mixtures. All samples, including Cp, can be applied in the separation of CO_2/CH_4 mixtures, but the K−Cp and Ca−Cp samples will probably be the most effective for the separation of N_2/O_2 and N_2/CH_4 mixtures.

References and Notes

(1) Breck, D. W. Zeolite *Molecular Sieves*; J. Wiley & Sons: New York, 1974; Chapter 1.
(2) Ming, D. W.; Dixon, J. B. *Clays Clay Minerals* **1987**, *35*, 463.
(3) Koyama, K.; Takeuchi, Y. *Z. Kristallogr.* **1977**, *145*, 216.
(4) Mumpton, F. A. In *Natural Zeolites: Occurrence, Properties, Use*; Sand, L. B., Mumpton, F. A., Eds.; Pergamon Press: New York, 1978.
(5) Tsisishvili, G. V.; Andronikashvili, T. G.; Kirov, G. N.; Filisova, L. D. *Zeolites*; Ellis Horwood: New York, 1992.
(6) Gradev, G.; Daiev, H. In *Bulgarian Natural Clinoptilolite Used as Cs^{137} Scavengers*; Scientific Meeting of Council for Economic Help, Kolobzeck, Poland, 1972.
(7) Minato, H.; Tamura, T. In *Natural Zeolites*: *Occurrence, Properties, Use*; Sand, L. B., Mumpton, F. A., Eds.; Pergamon Press: Oxford 1978; p 509.
(8) Galabova, I. M.; Haralampiev, G. A.; Alexiev, B. In *Natural Zeolites*: *Occurrence, Properties, Use*; Sand, L. B., Mumpton, F. A., Eds.; Pergamon Press: Oxford, 1978; p 431.
(9) Barrer, R. M.; Stuart W. I. *Proc. R. Soc.* **1959**, *A 249*, 464.
(10) Ayao, T.; Yoshihiro, M. J. *Soc. Mater. Sci. Jpn.* **1979**, *28*, 794.
(11) Frankiewicz, T. C.; Donnelly, R. G. In *Industrial Gas Separations*; Whyte, T. E., Jr., et al., Eds.; Am. Chem. Soc.: Washington, DC, 1983; p 213.
(12) Ackley, M. W.; Giese, R. F.; Yang, R. T. *Zeolites* **1992**, *12*, 780.
(13) Barrer, R. M. *J. Coll. Interface Sci.* **1966**, *21*, 415.
(14) Barrer, R. M. *Zeolite and Clay Minerals as Sorbents and Molecular Sieves*; Academic Press: London, 1978.
(15) Boniface, H.; Eriksson, R.; van Krusenstierna, O.; Ruthven, D.; Wester, M. European Patent 0132239, 1985.
(16) *Mineralogy and Geology of Natural Zeolites*; Mumpton, F. A., Ed.; Miner. Soc. Am.: Washington, DC, 1977; Chapter 4, 177.
(17) Powder Diffraction File (PDF), *International Centre for Diffraction Data*, U.S.A., 1993.
(18) Dubinin, M. M.; Astakhov, V. A. *Izv. Akad. Nauk, SSSR, Ser. Khim.* **1971**, *1* (5), in Russian.
(19) Dubinin, M. M.; Astakhov, V. A. *Adv. Chem.* **1971**, *102*, 69.
(20) Barrer, R. M.; Gibbons, R. M. *Trans. Faraday Soc.* **1965**, *61*, 948.
(21) Yang R. T. In *Gas Separation by Adsorption Processes*; Imperial College Press: 1997; Vol. 1; Chapter 1.
(22) Pauling, L. *The Nature of the Chemical Bond*, 3rd Ed.; Cornell University Press: Ithaca, NY, 1960; Chapter 13.
(23) *Handbook of Chemistry and Physics*, 63rd ed.; CRC Press: Boca Raton, FL, 1982−1983.
(24) Huheey, J. E. *Inorganic Chemistry: Principles of Structure and Reactivity*; University of Maryland, Harper & Row Publishers: New York, 1972; Chapter 4.
(25) Breck, D. W. *Zeolite Molecular Sieves*; J. Wiley & Sons: New York, 1974; Chapter 8.
(26) Ames, L. L. *Am. Mineral.* **1960**, *45*, 689.
(27) Hernández-Huesca, R.; Díaz, L.; Aguilar-Armenta, G. *Sep. Pur. Technol.* **1999**, *15*, 163.
(28) Shiralkar, V. P.; Kulkarni, S. B. *Zeolites* **1985**, *5*, 37.